HOKKAIDO UNIVERSITY

Title	A physics-informed neural network with subset simulation for structural reliability analysis
Author(s)	Wang, Weixi; Zhang, Wei-Heng; Thai, Huu-Tai et al.
Relation	Proceedings of the 10th International Symposium on Reliability Engineering and Risk Management (ISRERM 2026), June 28 - July 1, 2026, Sapporo, Japan
Citation	Proceedings of the 10th International Symposium on Reliability Engineering and Risk Management (ISRERM 2026)
Issue Date	2026-07-01
Doc URL	https://hdl.handle.net/2115/100441
Type	conference paper
File Information	C000084_1.pdf

Hokkaido University Collection of Scholarly and Academic Papers : HUSCAP

10th International Symposium on Reliability Engineering and Risk Management (ISRERM 2026),
28 June-01 July 2026, Sapporo, Japan
Kitahara, T., Miyamori, Y. & Beer, M. (editors)

A physics-informed neural network with subset simulation for structural reliability analysis

Weixi Wang[1, 2], Wei-Heng Zhang[2, *], Huu-Tai Thai[1] and Sebastian Thöns[2]

[1]*Department of Infrastructure Engineering, The University of Melbourne, Parkville, VIC 3010, Australia*
E-mail: weixiw1@student.unimelb.edu.au; tai.thai@unimelb.edu.au
[2]*Division of Structural Engineering, Lund University, Klas Anshelms väg 14, Lund 22363, Sweden*
E-mail: weiheng.zhang@kstr.lth.se; sebastian.thons@kstr.lth.se
**Corresponding Author*

Structural reliability analysis typically relies on extensive computations involving high-fidelity numerical models to evaluate the probability of failure, which makes conventional simulation-based approaches time-consuming and computationally expensive. Recent developments in Physics-Informed Neural Networks (PINNs) applied to computational mechanics provide a promising avenue for constructing cheap-to-evaluate surrogate models for structural reliability analysis. By explicitly incorporating random variables as additional inputs alongside spatial coordinates, PINNs learn the direct mapping between stochastic inputs and structural response, enabling simulation-free evaluation for the probability of failure. However, PINN-based surrogates trained with global sampling struggle to accurately capture complex limit state surfaces, highlighting the need for optimized sampling strategies. In this study, a structural reliability analysis framework is developed by integrating PINN with Subset Simulation (SS). The PINN surrogate acts as an effective alternative to numerical models for predicting structural behavior, while SS progressively guides samples toward the failure domain through a sequence of intermediate conditional levels with increasingly stringent failure thresholds. Numerical examples on three benchmarks further confirm that the proposed method delivers reliable assessment for the probability of failure and outperforms conventional PINNs based on Multilayer Perceptron (MLP).

Keywords: Structural reliability analysis, Physics-informed neural network, Subset simulation, Surrogate modeling

1 Introduction

Over the past century, the development of matrix methods, variational formulations, and computer-aided analysis has provided the foundation for modern computational structural mechanics (Kurrer 2018). As structural analysis extended from deterministic modelling to stochastic calculation and reliability assessment (Stefanou 2009), the computational cost of conventional numerical solvers such as the finite element method (FEM) increased significantly, because of the repeated evaluations required in such analyses. This challenge motivated the development of efficient model methods for structural reliability analysis, including First Order Reliability Method (FORM), Response Surface Method (RSM), and Polynomial Chaos Expansion (PCE) (Teixeira et al. 2021). More recently, deep neural networks (DNNs) have attracted widespread attention for complex engineering problems due to their powerful capability to learn high-dimensional nonlinear mappings (Thai 2022). Once trained, they can provide near-instantaneous inference and thus avoid repeated numerical simulations for new samples. Although DNN-based surrogate models have shown strong computational efficiency in structural reliability analysis (Afshari et al. 2022), their data-driven nature still depends heavily on training data, which are often generated from high-fidelity numerical simulations and can remain expensive to obtain. This has motivated increasing interest in incorporating prior physical knowledge into deep learning to improve physical consistency and reduce reliance on labeled data (Chen et al. 2021). Among these developments, Physics-Informed Neural Networks (PINNs), proposed by Raissi et al. (2019), are the most representative approaches. In PINNs, governing equations together with initial and boundary conditions are embedded into the loss function through automatic differentiation, enabling neural networks to construct mesh-free approximations guided by physical laws. PINNs have therefore become an active research direction in computational mechanics, with applications extending from fluid mechanics to heat transfer and solid mechanics (Hu et al. 2024). However, for a single forward mechanics problem, the training and tuning cost of PINNs still offers limited advantage over mature FEM. By contrast, in structural reliability analysis involving uncertainty, this upfront training cost can be offset by the large number of subsequent evaluations, making PINNs more attractive in practice.

An early study by Chakraborty et al. (2020) investigated the effectiveness of PINNs as simulation-free surrogate models for structural reliability analysis, in which the uncertain variables were introduced directly as inputs to the neural network. Subsequent studies can be mainly divided into two categories from the perspective of their role in reliability analysis. The first category integrates PINNs directly into the reliability analysis procedure. PINN-FORM proposed by Meng et al. (2023) is a representative example, where the design point search in FORM is incorporated into the training process and the reliability index is obtained together with the PDE solution. However, such methods remain dependent on FORM limitations becoming less accurate for non-normal distributions and for highly nonlinear failure surfaces, while the coupled training process can also become harder to tune. The second, which is more commonly discussed in the existing literature, uses PINNs as parametric responses or surrogates of the Limit State

Function (LSF), while the probability of failure is subsequently evaluated by external reliability algorithms. For this category, the predictive accuracy of the PINN surrogate near the limit state surfaces is crucial, since the probability of failure is highly sensitive to approximation errors in this region. This has consequently motivated a series of PINN surrogates with enhanced sample strategies, including AT-PINN-RA integrated with active learning (Zhang and Shafieezadeh 2022), PINN-IS coupled with importance sampling (Roy et al. 2024), and PINN-CE combined with the cross-entropy method (Liu et al. 2026). In these frameworks, the key is not simply to increase the number of training samples, but to guide sampling toward the most informative region near the limit state surface, so that the network is not dominated by more common sample combinations away from the failure region. A representative example is PINN-IS, which adopts a two-stage training strategy consisting of an initial coarse training stage to identify the Most Probable Point (MPP), followed by a second stage that focuses the training effort on an Importance Sampling (IS) distribution centered at that point. Although this approach has reported encouraging accuracy for classical structural benchmark problems, it also exposes several limitations. First, enhanced sampling in the second stage depends on the MPP identified in the first stage. If this estimate is biased, the subsequent training may be directed toward an incorrect failure region. Second, the refined samples introduced in the second stage often differ substantially from those used in the initial stage, leading to a pronounced distribution shift that can make the training process less stable.

To address these limitations, this study proposes a PINN-SS framework for structural reliability analysis, in which SS is used to generate more informative training samples for PINN surrogates. Instead of refining the network around an estimated MPP, the proposed framework progressively enriches the training samples through a sequence of intermediate subsets, thereby reducing the risk of bias caused by an inaccurate initial estimate while enabling a smoother transition toward the failure region and a more robust training process. In terms of network architecture, the recently proposed Kolmogorov-Arnold Network (KAN) is adopted to replace the Multilayer Perceptron (MLP) commonly used in PINNs, with the aim of improving the approximation of parameterized mappings involving uncertain inputs. The remainder of this paper is organized as follows: Section 2 presents the KAN-based computational framework; Section 3 introduces the SS-based enhanced sample strategy; Section 4 validates the proposed method through three classical benchmark problems; Finally, Section 5 summarizes the main findings, discusses the limitations of the present surrogate, and outlines possible directions for future research.

2 KAN-based PINN Framework

Conventional PINN frameworks are typically built on the MLP. In this architecture, normalized inputs are propagated through multiple hidden layers to predict target physical quantities, while each layer performs an affine transformation followed by a nonlinear activation. Specifically, for the l_{th} to l_{th+1} layer, the propagation can be written as

$$x_j^{(l+1)} = \sigma\left(\sum_{i=1}^{n_l} W_{ji}^{(l)} x_i^{(l)} + b_i^{(l)} \right), \tag{1}$$

where W and b are the trainable weights and biases, and $\sigma(\cdot)$ represents the activation function, commonly chosen as the hyperbolic tangent or ReLU. This simple form of feedforward mapping with a fixed activation gives MLP strong approximation capability and efficient function representation. However, when uncertain inputs introduce multi-scale or highly nonlinear features into mappings, its performance can become sensitive to network size and hyperparameter choices.

Recently, the KAN proposed by Liu et al. (2025), has attracted considerable attention as a promising alternative to conventional MLP architecture. The key innovation of KAN is that it replaces the fixed activation functions in MLP with learnable univariate functions defined on network edges. Accordingly, the mapping in a KAN can be written as

$$x_j^{(l+1)} = \sum_{i=1}^{n_l} \phi_{ji}^{(l)} x_i^{(l)}, \quad \phi_{ji}^{(l)}(x) = \sum_{m=1}^{M} c_{ji,m}^{(l)} B_m(x) \tag{2}$$

where $\phi(\cdot)$ is the learnable univariate function, represented as a linear combination of spline basis function $B(\cdot)$ with trainable coefficient c. By parameterizing nonlinear mappings on network edges, KAN can provide a more flexible functional representation with a more compact network architecture and potentially more stable training. However, some studies have also reported that KAN can be significantly slower to train than conventional MLPs, partly because effective training strategies and dedicated optimizers remain insufficiently developed (Wang et al., 2024).

Figure 1 shows the workflow of the proposed PINN surrogate framework for structural reliability analysis. Unlike PINN frameworks that are developed for a single deterministic structural analysis, the present framework introduces uncertain variables directly into the network inputs so that a parameterized surrogate model can be constructed over the joint input space. A KAN with hidden size [5, 5]. grid size g = 5, and polynomial order k = 3 is adopted as the surrogate approximator, instead of the conventional MLP-based DNN. Although training KAN is generally more time-consuming, this drawback is less critical in structural reliability analysis, where the trained surrogate is used for a large number of repeated evaluations. In this setting, the one-time training cost is amortized, while both KAN- and MLP-based surrogates can provide rapid inference once trained, making the performance of surrogates more important. The network is used to predict the structural response, and its output field is further modified through a hard constraint so

that the prescribed boundary conditions are satisfied exactly. This design avoids the introduction of boundary penalty terms into the loss function, thereby improving training stability and eliminating the need for additional weight tuning. Automatic differentiation is then used to compute the required derivatives and construct the residuals of the governing equations, which define the physics-informed loss for training. Once sufficiently trained, the surrogate is used to evaluate the LSF for Monte Carlo Simulation (MCS) in the random variable space, from which the probability of failure is estimated. All subsequent numerical studies are conducted within this PINN framework, and the specific training strategies and hard constraint formulations are presented in the corresponding subsections.

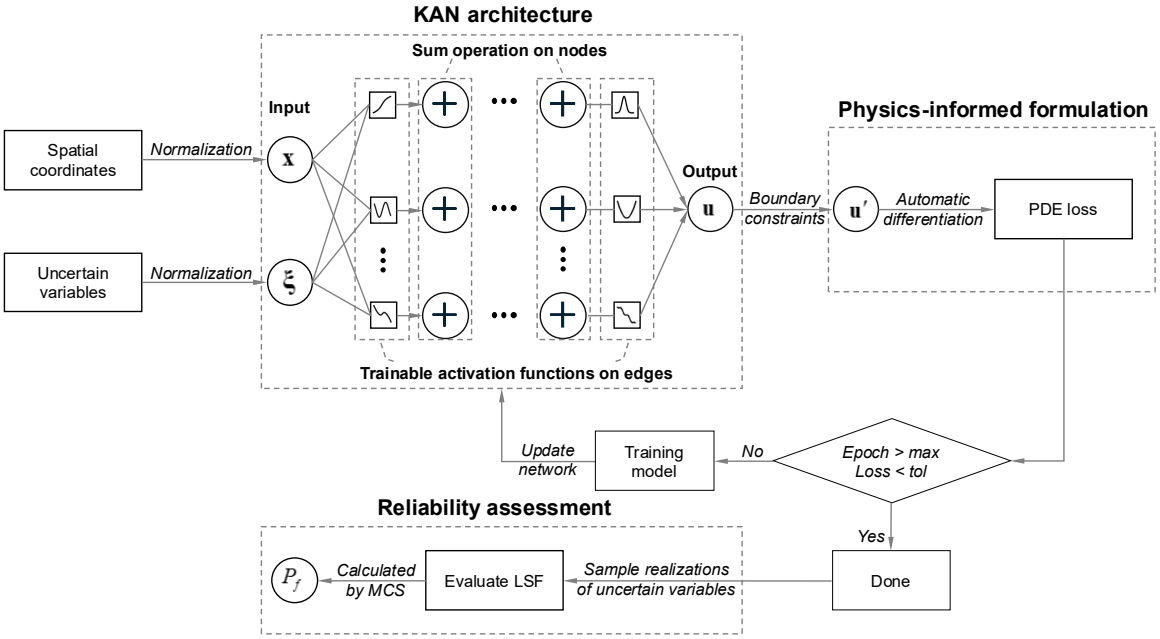

Figure 1. Workflow of the proposed KAN-based PINN framework for structural reliability analysis.

3 SS-based Sample Strategy

In structural reliability analysis, the local accuracy of a PINN surrogate near the limit state surface is more important than its global accuracy over the entire input space. However, directly concentrating training samples around a preliminarily identified failure boundary is generally unreliable, since errors in the early-stage surrogate can bias the estimated limit state surface and an overly localized sampling can reduce training robustness. For this reason, this study proposed an enhanced sampling strategy based on SS. Specifically, an initial PINN surrogate is first trained using globally distributed samples, and its predicted LSF values are then used to define a sequence of nested subsets with gradually decreasing intermediate thresholds. Conditional samples are generated within each subset so that the samples progressively move toward the limit state surface. The corresponding mathematical formulation is given as follows.

For a structural system with uncertain variables ξ, the probability of failure is defined as

$$P_f = P\left\{g\left(\xi\right) \le 0\right\}, \tag{3}$$

where $g\left(\xi\right)$ is the LSF. Based on the initial PINN surrogate, a sequence of nested subsets is constructed as

$$F_j = \left\{\xi : \hat{g}\left(\xi\right) \le b_j\right\},\ \ j = 1,2,...,m, \tag{4}$$

where $\hat{g}\left(\xi\right)$ is the predicted LSF value. These subsets satisfy $F_1 \supset F_2 \supset ... \supset F_m$, where b_j is the intermediate threshold at the j_{th} subset level. It is determined from predicted LSF values of samples generated at previous level as,

$$b_j = \hat{g}_{(ns)}^{(j-1)},\ \ n_s = p_0 N, \tag{5}$$

where n_s is the prescribed conditional probability level, and N is the total number of samples per level. Starting from the retained samples, conditional samples are generated by a correlated Gaussian Markov random walk,

$$\tilde{\xi}^{(j,l)} = a\xi^{(j,l-1)} + \sqrt{1-a^2}\, z^{(j,l)},\ \ z^{(j,l)} \sim \mathcal{N}\left(0,1\right), \tag{6}$$

where a controls the correlation between successive samples, only the samples satisfying $\hat{g}\left(\tilde{\xi}^{(j,l)}\right) \le b_j$ are retained.

Figure 2 illustrates the SS-based sample generation process in a two-dimensional uncertainty space with Z1 and Z2 as the uncertain variables. Starting from the initial global sample set, the generated samples progressively move toward the black curve, which represents the limit state surface. The selected samples from different subset levels are then combined with the retained original global samples to form the updated training set, with the number of selected samples at each level determined by the corresponding intermediate threshold b,

$$\mathcal{D}^{\text{new}} = \mathcal{D}_0^{\text{sel}} \cup \bigcup_{l=1}^{L} \mathcal{D}_l^{\text{sel}}, \quad N_l = \frac{\sum_{j=1}^{L} b_j - b_l}{(L-1)\sum_{j=1}^{L} b_j} N_{\text{SS}}, \tag{7}$$

where $\mathcal{D}_0^{\text{sel}}$ denotes the retained samples from level 0. And $\mathcal{D}_l^{\text{sel}}$ denotes the selected samples from the l_{th} subset level, and L is the final subset level. Here, N_l is the number of samples selected from the corresponding level, while N_{ss} is the total number of samples assigned to all subset levels.

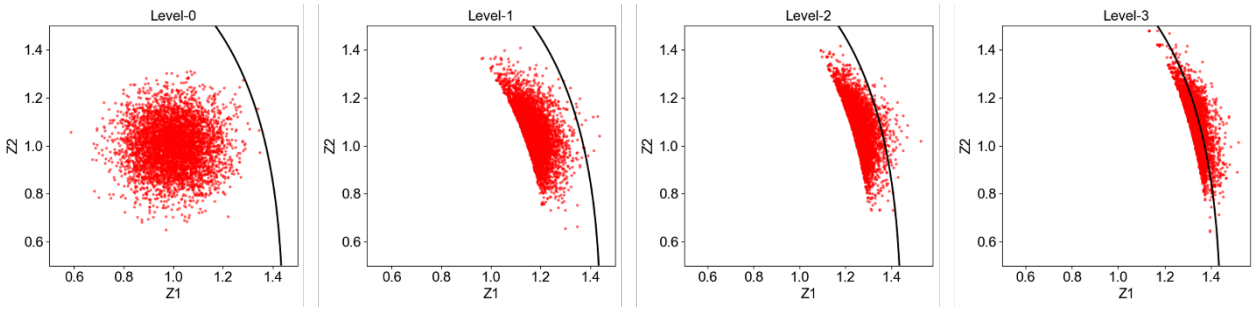

Figure 2. Schematic illustration of the evolution of SS-generated samples in a two-dimensional uncertainty space.

4 Numerical Study

Based on the above foundations, a two-stage PINN-SS surrogate model is proposed for structural reliability analysis. In the first stage, an initial surrogate is trained using globally distributed samples to capture the overall response over the uncertain variable space. In the second stage, SS is employed to enrich the collocation points with samples concentrated near the limit state surface, and the surrogate is further refined to improve prediction accuracy in this region. To validate the effectiveness of the proposed surrogate model, three classical benchmark cases are considered. Their geometries and parameter settings are adopted from the work by Roy et al. (2024), with only the parameter magnitudes scaled to practical engineering ranges.

4.1 *A straight bar subjected to an axial load*

Figure 3 shows a straight bar subjected to an axial tensile load, with a total length of L = 5m and a fixed left end. The uncertain variables considered are the load F, the cross-sectional area A, and Young's modulus E, which are assumed to follow the triangular distributions listed in Table A.1 from Appendix A, consistent with those adopted in Roy et al. (2024). The governing equation and boundary condition for this bar are as follows,

$$\frac{du}{dx} - \frac{F}{AE} = 0; \quad u = 0 \text{ at } x = 0, \tag{8}$$

where the neural network output is modified as $u' = (x/L) \cdot u(x, F, A, E)$ using such hard constraint. The LSF is defined as $g = u_{\max} - u_{(x=5)}$, where $u_{\max}$ is the maximum allowable displacement, taken as 4.5mm in this case.

In the first stage of PINN-SS, 1,000 sample points generated by Latin hypercube sampling (LHS) in the joint input space of (x, F, A, E) are used to train an initial KAN surrogate for 5,000 iterations with a learning rate of 0.001, and the network with the minimum physical loss is retained as the baseline model. In the second stage, SS is performed with p_0 = 0.1, a = 0.8 in this study. Starting from 20,000 samples in level 0, the most critical 10% are selected as seeds, and each seed is propagated through 10 random-walk steps to generate conditional samples for the following levels. The surrogate is then further refined for another 5,000 iterations using 1,000 resampled collocation points per iteration, and the network with the minimum loss is adopted as the final PINN-SS model.

In this case, a direct MCS with 10^{10} samples was first performed based on the analytical solution, yielding a probability of failure P_f of 1.842×10^{-6} with a Coefficient of Variation (COV) of 0.74%, which was taken as the reference value for this validation. Based on the trained surrogates, 10 independent MCS runs with 10^8 samples in each run are carried out to evaluate the LSF and estimate the probability of failure. To verify the advantage of the proposed method, further comparisons are conducted with a single-stage PINN model and an MLP-based PINN-SS model. Both

benchmark surrogate models employ an MLP with five hidden layers, 50 neurons per layer, and the *tanh* activation function. The single-stage PINN is trained for 10,000 iterations, while the MLP-based PINN-SS follows the same two-stage setting as the proposed model. As shown in Figure 4, the proposed KAN-based PINN-SS yields failure probability estimates in the closest agreement with the MCS reference, while exhibiting a more stable performance than the MLP-based counterparts. Table 1 summarizes the mean failure probabilities, standard deviations, and relative errors against MCS reference for the three surrogate models based on 10 independent MCS runs in this bar example.

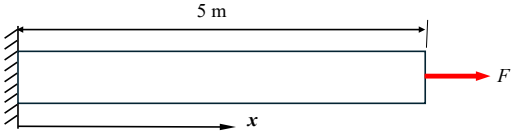

Figure 3. Schematic of a straight bar subjected to an axial load.

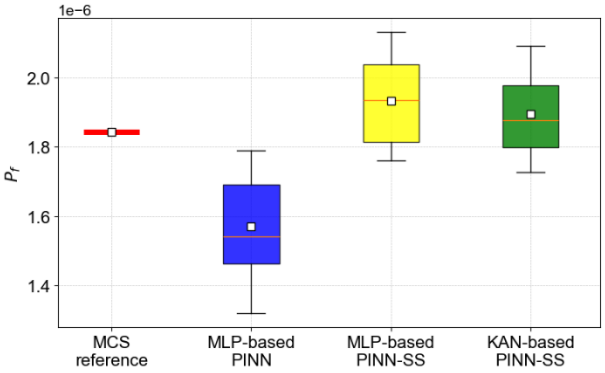

Figure 4. Failure probability estimates for the straight bar from 10 independent MCS using different surrogate methods.

Table 1. Comparison of three surrogate models over 10 independent MCS runs for the straight bar.

Reliability approach	$\overline{P}_f$	Standard deviation	$\overline{P}_f$ error (%)
MCS Reference	1.842×10^{-6}	-	-
MLP-based PINN	1.569×10^{-6}	1.489×10^{-7}	14.82
MLP-based PINN-SS	1.931×10^{-6}	1.337×10^{-7}	4.83
KAN-based PINN-SS	1.893×10^{-6}	1.293×10^{-7}	2.77

4.2 *A cantilever beam subjected to a uniformly distributed load*

Figure 5 shows a cantilever beam under a uniformly distributed load, with a total length of L = 2m. The uncertain variables considered are the load amplitude w, Young's modulus E, and the moment of inertia I, which are assumed to follow the truncated normal distributions listed in Table A.2. The governing equation is as follows,

$$EI\frac{d^2u}{dx^2}-\frac{w(L-x)^2}{2}=0;\quad u=0 \text{ at } x=0;\quad \frac{du}{dx}=0 \text{ at } x=0, \tag{9}$$

where the neural network output is modified by the hard constraint as $u'=(x/L)^2\cdot u(x,F,A,E)$. The LSF is defined as $g=u_{\max}-u_{(x=2)}$, where $u_{\max}$ is the maximum allowable displacement, taken as 4.0×10^{-3}m in this case.

A reference failure probability of 4.328×10^{-6} was first obtained from an MCS with 10^{10} samples based on the analytical solution, with an associated COV of 0.48%. The three surrogate models were then evaluated under the same training setting using 10 independent MCS runs with 10^8 samples, and the corresponding P_f estimates are shown in the boxplots in Figure 6. Table 2 further reports the mean failure probability estimated from the 10 runs, together with its relative error with respect to reference value and the corresponding standard deviation.

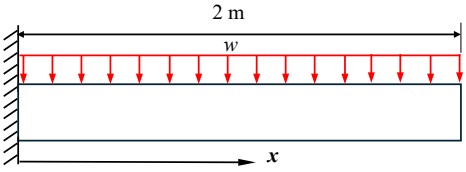

Figure 5. Schematic of a cantilever beam subjected to a uniformly distributed load.

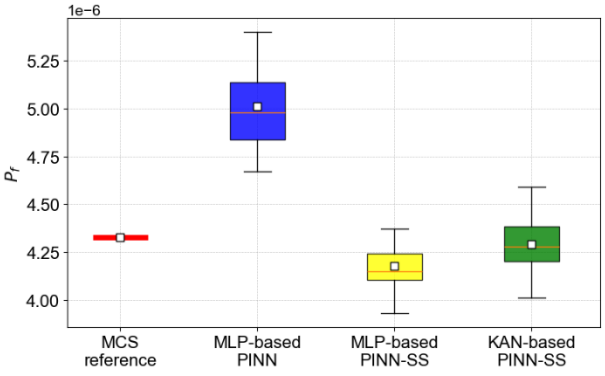

Figure 6. Failure probability estimates for the cantilever beam from 10 independent MCS using different surrogate methods.

Table 2. Comparison of three surrogate models over 10 independent MCS runs for the cantilever beam.

Reliability approach	$\overline{P}_f$	Standard deviation	$\overline{P}_f$ error(%)
MCS Reference	4.328×10^{-6}	-	-
MLP-based PINN	5.011×10^{-6}	2.385×10^{-7}	15.76
MLP-based PINN-SS	4.177×10^{-6}	1.656×10^{-7}	3.49
KAN-based PINN-SS	4.291×10^{-6}	1.636×10^{-7}	0.85

4.3 *A thin square plate subjected to a sinusoidally distributed load*

Figure 7 shows a simply supported thin square plate under a sinusoidal load, with a thickness h = 0.05m. The uncertain variables considered are the load amplitude q_0, Young's modulus E, and Poisson's ratio ν, which are assumed to follow the truncated normal distributions listed in Table A.3. The governing equation is as follows,

$$\frac{Eh^3}{12(1-\nu^2)}\left(\frac{\partial^4\omega}{\partial x^4}+2\frac{\partial^4\omega}{\partial x^2\partial^2 y}+\frac{\partial^4\omega}{\partial y^4}\right)=q_0\sin x\sin y, \tag{10}$$

where the neural network output is modified by the hard constraint as $\omega'=(\sin x\sin y)\cdot(x,q_0,E,\nu)$. The LSF is defined as $g=\omega_{\max}-\omega_{(x=\pi/2,\,y=\pi/2,)}$, where $\omega_{\max}$ is the maximum allowable deflection, taken as 1.5×10^{-2}m.

The reference P_f of 1.472×10^{-5} was first obtained from an MCS with 10^9 samples based on the analytical solution, with an associated COV of 0.82%. The surrogates were then evaluated under the same training setting using 10 independent MCS runs with 10^7 samples, and comparisons are shown Figure 8 and Table 3. The results from all numerical studies consistently demonstrate that SS improves the estimation accuracy for small failure probabilities. In addition, the KAN-based surrogate exhibits the best overall performance, with all relative errors remaining within 3%.

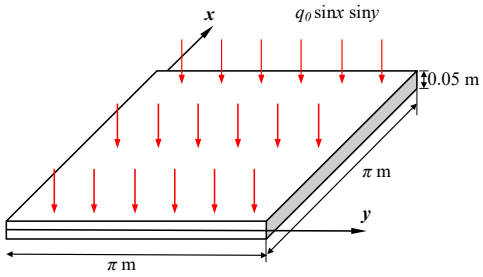

Figure 7. Schematic of a thin square plate with a sinusoidally distributed load.

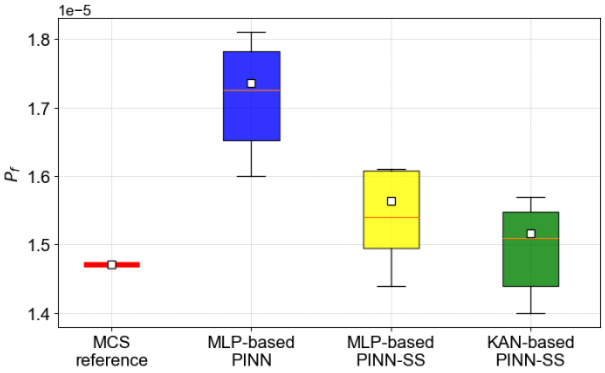

Figure 8. Failure probability estimates for the thin square plate from 10 independent MCS using different surrogate methods.

Table 3. Comparison of three surrogate models over 10 independent MCS runs for the thin square plate.

Reliability approach	$\overline{P}_f$	Standard deviation	$\overline{P}_f$ error(%)
MCS Reference	1.472×10^{-5}	-	-
MLP-based PINN	1.736×10^{-5}	1.230×10^{-6}	17.93
MLP-based PINN-SS	1.564×10^{-5}	1.045×10^{-6}	6.25
KAN-based PINN-SS	1.516×10^{-5}	1.004×10^{-6}	2.98

5 Conclusion

In summary, this study develops a cheap-to-evaluate PINN-SS surrogate for structural reliability analysis and validates its effectiveness on three benchmarks with small failure probabilities. The key innovation is the incorporation of the conditional sample generation mechanism of SS into the PINN sampling process, which progressively drives the collocation points toward the limit state surface rather than relying only on global sampling or sampling concentrated around MPP. This enhanced sampling strategy results in more robust training and more accurate prediction of the limit state surface. Furthermore, the results show that, for input spaces involving multi-scale uncertain variables, KAN can provide higher predictive accuracy than the conventional MLP due to its stronger local representation capability. However, the present study is limited to simple elastic problems, while the two-stage training framework remains inefficient. Future work will focus on adaptive SS-based training, sophistications to structural reliability problems with geometric and material nonlinearities, and further evaluation in terms of training convergence and cost.

Acknowledgments

This work was supported by the Australian Research Council (ARC) under Future Fellowship Grant (FT200100024). The financial support is gratefully acknowledged. The authors also gratefully acknowledge support from the Lund University GloHub Doctoral Student Mobility Initiative.

Appendix A. The distribution parameters of random variables used in this study

Tables A.1–A.3 summarize the distribution parameters of the random variables for the three numerical examples, which are adopted from the work of Roy et al. (2024).

Table A.1. The triangular distribution parameters of random variables for the straight bar.

Random variable	Mean	Standard deviation	Lower bound	Upper bound
F (N)	1.00×10^{5}	0.10×10^{5}	7.55×10^{5}	12.45×10^{5}
A (m^2)	1.00×10^{-2}	0.10×10^{-2}	0.755×10^{-2}	1.245×10^{-2}
E (N/m^2)	2.06×10^{11}	0.15×10^{11}	1.693×10^{11}	2.427×10^{11}

Table A.2. The truncated normal distribution parameters of the random variables for the cantilever beam.

Random variable	Mean	Standard deviation	Lower bound	Upper bound
w (N/m)	2.00×10^{3}	0.20×10^{3}	1.40×10^{3}	2.60×10^{3}
E (N/m^2)	2.00×10^{11}	0.15×10^{11}	1.55×10^{11}	2.45×10^{11}
I(m^4)	1.00×10^{-5}	0.10×10^{-5}	0.70×10^{-2}	1.30×10^{-2}

Table A.3. The truncated normal distribution parameters of random variables for the thin square plate.

Random variable	Mean	Standard deviation	Lower bound	Upper bound
q_0 (N/m^2)	0.5×10^{6}	0.2×10^{6}	0.0	1.0×10^{6}
E (N/m^2)	2.0×10^{-11}	0.2×10^{-11}	1.4×10^{-11}	2.6×10^{-11}
v	0.3	0.1	0.0	0.6

References

Afshari, S. S., Enayatollahi, F., Xu, X. and Liang, X., Machine learning-based methods in structural reliability analysis: A review, *Reliab. Eng. Syst. Saf.*, 219, 108223, 2022.

Chakraborty, S., Simulation free reliability analysis: A physics-informed deep learning based approach, *arXiv preprint arXiv:*2005.01302*,* 2020.

Chen, Z., Liu, Y. and Sun, H., Physics-informed learning of governing equations from scarce data, *Nat. Commun.*, 12(1), 6136, 2021.

Hu, H., Qi, L. and Chao, X., Physics-informed neural networks (PINN) for computational solid mechanics: Numerical frameworks and applications, *Thin-Walled Struct.*, 205, 112495, 2024.

Kurrer, K.-E., *The History of the Theory of Structures: Searching for Equilibrium*, 2nd ed., Ernst & Sohn, Berlin, 2018.

Liu, B., Chen, Z., Chen, G., Pan, Q., Guo, G., Liu, D., Li, X. and Gan, X., Reliability analysis using adaptive physics-informed neural network with cross-entropy optimization, *Appl. Math. Model.*, 153, 116627, 2026.

Liu, Z., Wang, Y., Vaidya, S., Ruehle, F., Halverson, J., Soljačić, M., Hou, T. Y. and Tegmark, M., *KAN: arXiv preprint arXiv:*2404.19756, 2025.

Meng, Z., Qian, Q., Xu, M., Yu, B., Yıldız, A. R. and Mirjalili, S., PINN-FORM: A new physics-informed neural network for reliability analysis with partial differential equation, *Comput. Methods Appl. Mech. Engrg.*, 414, 116172, 2023.

Raissi, M., Perdikaris, P. and Karniadakis, G. E., Physics-informed neural networks: A deep learning framework for solving forward and inverse problems involving nonlinear partial differential equations, *J. Comput. Phys.*, 378, 686-707, 2019.

Roy, A., Chatterjee, T. and Adhikari, S., A physics-informed neural network enhanced importance sampling (PINN-IS) for data-free reliability analysis, *Probab. Eng. Mech.*, 78, 103701, 2024.

Stefanou, G., The stochastic finite element method: Past, present and future, *Comput. Methods Appl. Mech. Engrg.*, 198, 1031-1051, 2009.

Teixeira, R., Nogal, M. and O'Connor, A., Adaptive approaches in metamodel-based reliability analysis: A review, *Struct. Saf.*, 89, 102019, 2021.

Thai, H.-T., Machine learning for structural engineering: A state-of-the-art review, *Structures*, 38, 448-491, 2022.

Wang, Y., Sun, J., Bai, J., Anitescu, C., Eshaghi, M. S., Zhuang, X., Rabczuk, T. and Liu, Y., Kolmogorov-Arnold-Informed neural network: A physics-informed deep learning framework for solving forward and inverse problems based on Kolmogorov-Arnold Networks, *Comput. Methods Appl. Mech. Engrg.*, 433, 117518, 2025.

Zhang, C. and Shafieezadeh, A., Simulation-free reliability analysis with active learning and Physics-Informed Neural Network, *Reliab. Eng. Syst. Saf.*, 226, 108716, 2022.